Experimental measurement of biofilm in a heat exchanger
by Douglas Wayne Heal

A thesis submitted in partial fulfillment of the requirements for the degree of Master of Science in Mechanical Engineering
Montana State University


Abstract:
The purpose of this research, the experimental measurement of a biofilm in a heat exchanger, was to determine the relationship between the biofilm thickness and certain flow parameters. Four test runs were conducted using four different test sections to determine the effect a biofilm produces on the friction factor, the wall shear stress, and the pressure fluctuations in a heat exchanger. The change in the friction factor and the growth of the biofilm approximated the theoretical work, with slight discrepancies in the induction time and maximum values at the conclusion of each test run. The results of the wall shear stress were promising, with the maximum wall shear stress similar for all four test runs in all four flow loops. The pressure fluctuations proved inconclusive in the research, with a random variation of frequencies occurring throughout the investigation. The results of the detachment phase showed a linear relationship between the test parameters and the fluid velocity for the range tested.

# EXPERIMENTAL MEASUREMENT OF BIOFILM IN A HEAT EXCHANGER

by

Douglas Wayne Heal

A thesis submitted in partial fulfillment
of the requirements for the degree

of

Master of Science

in

Mechanical Engineering

MONTANA STATE UNIVERSITY
Bozeman, Montana

June, 1989

**APPROVAL**

**of a thesis submitted by**

**Douglas Wayne Heal**

**This thesis has been read by each member of the thesis committee and has been found to be satisfactory regarding content, English usage, format, citations, bibliographic style, and consistency, and is ready for submission to the College of Graduate Studies.**

June 28, 89 — Date
Harry W. Towns — Chairperson, Graduate Committee

**Approved for the Major Department**

6-29-89 — Date
Head, Major Department

**Approved for the College of Graduate Studies**

July 5, 1989 — Date
Henry L Parsons — Graduate Dean

## STATEMENT OF PERMISSION TO USE

In presenting this thesis in partial fulfillment of the requirements for a master's degree at Montana State University, I agree that the Library shall make it available to borrowers under rules of the Library. Brief quotations from this thesis are allowable without special permission, provided that accurate acknowledgement of the source is made.

Permission for extensive quotation from or reproduction of this thesis may be granted by my major professor, or in his/her absence, by the Dean of Libraries when, in the opinion of either, the proposed use of the material is for scholarly purposes. Any copying or use of the material in this thesis for financial gain shall not be allowed without my written permission.

Signature Douglas Heal

Date 6-30-89

## ACKNOWLEDGEMENTS

The author is indebted to the following persons for their assistance in this investigation.

Carl Hoerger, for his guidance and encouragement throughout all phases of the experimentation.

Harry Townes, for his advice and assistance in completing the project.

Pat Vowell and Gordon Williamson, for their advice and assistance in the construction and design of the laboratory equipment.

Alan George, for his advice and assistance in the experimentation.

The staff of the Mechanical Engineering Department at Montana State University for their assistance in all aspects of the experimentation.

The National Science Foundation, for their financial assistance throughout the project. Grant No. CBT-8707821

Deanna Walker, for her assistance in proofreading the final version of the thesis.

# TABLE OF CONTENTS

TABLE OF CONTENTS-Continued

## LIST OF TABLES

## LIST OF FIGURES

LIST OF FIGURES--Continued

LIST OF FIGURES--Continued

## NOMENCLATURE

| Symbol | Description |
|---|---|
| A | Area |
| $A_c$ | Cross-Sectional Area |
| C | Circumference |
| $c_f$ | Coefficient of Friction |
| D | Diameter |
| DMS | Data Monitoring Software |
| DO | Dissolved Oxygen |
| e | Average Depth of Roughness |
| e/D | Relative Roughness |
| F | Degrees Fahrenheit |
| f | Friction Factor |
| $f_{10,000}$ | Friction Factor for a Reynolds number of 10,000 |
| ft | Feet |
| FFT | Fast Fourier Transform |
| g | Acceleration Due to Gravity |
| gm | Gram |
| GPM | Gallons per Minute |
| $h_f$ | Head Loss Due to Friction |
| hr | Hour |
| Hz | Cycles per Second |

## NOMENCLATURE

| Symbol | Description |
|---|---|
| in | Inches |
| k | Average Depth of Roughness |
| Khz | Kilocycles per second |
| L | Length |
| Lbf | Pounds-Force |
| m | Meter |
| mm | Millimeters |
| MHz | Megacycles per Second |
| min | Minute |
| MSU | Montana State University |
| $\dot{m}$ | Mass Flow Rate |
| P | Pressure |
| PPM | Parts per Million |
| PSI | Pounds-Force per Square Inch |
| $P_{dyn}$ | Dynamic Pressure |
| r | Radius |
| Re | Reynolds number |
| s | Seconds |
| T | Temperature |
| t | Time |

## NOMENCLATURE

| Symbol | Description |
|---|---|
| TFM | Turbine Flowmeter |
| $u_{()}$ | Uncertainty |
| v | Velocity |
| v. | Versus (in comparison to) |
| z | Elevation |
| $\mu$ | Absolute Viscosity |
| $\gamma$ | Specific Weight |
| $\pi$ | 3.14 |
| $\sigma$ | Standard Deviation |
| $\tau_o$ | Wall Shear Stress |
| $\tau_{10,000}$ | Wall Shear Stress for a Reynolds number of 10,000 |
| $\nu$ | Kinematic Viscosity |
| d( ) | Differential Quantity |
| $\rho$ | Mass Density |

## ABSTRACT

The purpose of this research, the experimental measurement of a biofilm in a heat exchanger, was to determine the relationship between the biofilm thickness and certain flow parameters. Four test runs were conducted using four different test sections to determine the effect a biofilm produces on the friction factor, the wall shear stress, and the pressure fluctuations in a heat exchanger. The change in the friction factor and the growth of the biofilm approximated the theoretical work, with slight discrepancies in the induction time and maximum values at the conclusion of each test run. The results of the wall shear stress were promising, with the maximum wall shear stress similar for all four test runs in all four flow loops. The pressure fluctuations proved inconclusive in the research, with a random variation of frequencies occurring throughout the investigation. The results of the detachment phase showed a linear relationship between the test parameters and the fluid velocity for the range tested.

# CHAPTER 1

## INTRODUCTION

One of the major problems facing industry today is the effect of fouling upon heat exchangers. Fouling refers to the formation of an unwanted substance on the surface of a heat exchanger. This formation, or film, can greatly reduce the overall efficiency of the heat exchanger by lowering the heat transfer rate and increasing the pressure drop within the heat exchanger. As the film continues to enlarge, it will continue to lower the efficiency and may eventually restrict the flow of fluid in the heat exchanger completely. The annual cost from this lowered efficiency due to fouling has been estimated by Marner and Suiter [1] to be four to seven billion dollars per year for the United States industrial sector alone.

There are several types of fouling which may affect a heat exchanger. Precipitation fouling occurs when soluble salts which are suspended in the heat exchanger fluid precipitate onto the heat exchanger surface. Particle fouling occurs when suspended particles accumulate on the inside of the heat exchanger. Chemical reaction fouling is caused by the attachment of the products of a chemical reaction onto the heat exchanger surface. Corrosion fouling is caused by the deposition of corrosion products onto the heat exchanger surface. Finally there is biological fouling, or biofouling, which results from the attachment and growth of microorganisms on the heat exchanger surface.

According to Strauss and Puckorius [2] the two recognized forms of industrial biofouling are microbiological fouling of heat exchangers and macrobiological fouling of intake and discharge canals. The former is caused by both plant and animal organisms such as algae and bacteria. The latter stems primarily from invertebrate life such as mussels or clams. This research was concerned exclusively with the investigation of the first, microbiological fouling.

Currently no satisfactory method exists to control the effect of the fouling in heat exchangers. One method is simply to wait until the heat exchanger performance has been substantially reduced, which is indicated by a decrease in the temperature rise across the heat exchanger surface or by reduced condenser vacuum, and then to stop the process and physically remove the deposits. These indicators are very poor in reflecting the fouling occurring within the heat exchanger and irreparable damage may have already occurred before the indicators show that a problem exists. A second method is to add to the heat exchanger fluid chemicals which inhibit any type of potential growth. Periodic chlorination of the water is a common example of this method. Unfortunately, government regulations have severely limited the level of chlorine in heat exchanger fluid discharges, which in turn makes this procedure illegal in many areas. Velocity excursions may be used to remove some of the fouling, but this method does not remove the fouling from the heat exchanger completely and the deposition from fouling quickly returns, causing the efficiency of the heat exchanger to be reduced again. Mechanical cleaning may be used, but the cost of this type of removal is high. Recently a thermal

backwash technique has been experimented with at power plants on the West and East coasts. Thermal backwash, however, must be done frequently enough to kill marine organisms in the juvenile stage. This technique's success depends on the organisms' acclimatization temperatures and thus has met with little success when implemented.

The above control strategies have three major weaknesses according to Turakhia [3]:

1. Process instrumentation is not accurate enough to adequately sense fouling. It may give erroneous information as to the presence of fouling, and by the time that a deposit has been sensed, it may be too late to control it by methods other than stopping the process and physically cleaning the heat exchanger.

2. Indirect methods of determining the cause of the deposit may suggest a variety of potential factors. Often an effective treatment program can only be determined by trial and error.

3. Diagnosis of the problem and prescription of the treatment program require a knowledge of not only fouling in general, but also the past history of the particular treatment. Such knowledge must be developed over time for each application because of the complex interactions which may contribute to fouling.

The problem of determining the type of fouling occurring within the heat exchanger also poses a dilemma. It may be evident that the heat exchanger has a film buildup, but identification of the film may be difficult if not impossible.

The biofilm composition may be determined visually, but it is then again necessary to shut the heat exchange process down, since shutting down is costly, this method is not appealing. This leaves examination of the heat transfer fluid and past consideration of the heat exchanger as the predominant methods for biofilm identification. These methods are inexact and unreliable in most applications.

The current research investigated the possibility of deriving a relationship between the biofilm thickness and various flow parameters such as the friction factor and the wall shear stress. This correlation would then be used to create a fouling "monitor" which would be capable of taking continuous data on the biofilm. The monitor would then use the information to create a base of information to help in determining the biofilm thickness and type. Corrective measures could then be implemented by the individual to remove the biofilm while the heat exchanger is still in operation.

# CHAPTER 2

## REVIEW OF PREVIOUS FINDINGS

### Summary of Previous Findings

Although there has been a great deal of investigation into the effects of surface roughness on fluid flow, most previous work was based upon the assumption of a uniform surface roughness and a constant inside pipe diameter. Unfortunately, a biofilm is constantly changing its physical characteristics as it matures and grows.

Some of the earliest work in fluid dynamics was done by Sir Issac Newton who theorized that for straight and parallel motion of a fluid, the tangential stress, $\tau$, between the two adjacent layers was proportional to the velocity gradient, $\partial u$, in a direction perpendicular to the layers, $\partial y$. This gives the relationship:

$$\tau = \mu \frac{\partial u}{\partial y} \tag{1}$$

The coefficient of proportionality $\mu$ is now known as the absolute viscosity of the fluid.

In 1840, G. H. L. Hagen [4] and J. L. M. Poiseuille [5] studied laminar flow in circular pipes. Hagen experimented with the flow of water through small brass tubes. His results showed that loss of head for a given length of pipe

was directly proportional to the rate of flow and inversely proportional to the diameter of the tube to the fourth power. Poiseuille also arrived at the same conclusion working with small capillary tubes. This relationship between the pressure loss and flow parameters was termed the Hagen-Poiseuille relationship and is defined by the equation:

$$p_1 - p_2 = 8\mu l \frac{Q}{\pi R^4} \tag{2}$$

In 1883, Osborne Reynolds [6] investigated the characteristics of laminar and turbulent flow. Reynolds performed a series of experiments in which dye was injected into water flowing through a glass pipe. Reynolds experiments and his analytical work showed that the nature of pipe flow depends on a dimensionless parameter which he called the Reynolds number. This parameter was determined by the relationship:

$$Re = \frac{\rho u_m D}{\mu} \tag{3}$$

where $\rho$ is the mass density of the fluid, $u_m$ is the mean velocity of the fluid, D is the hydraulic diameter, and $\mu$ is the absolute viscosity of the fluid. With his experimental and analytical work he showed that the Reynolds number was characteristic to both laminar and turbulent flow. From his work, he concluded that the transition between laminar and turbulent flow occurred at a Reynolds number of 2000. If special precautions were taken not to disturb the fluid, Reynolds found that this transition period was delayed to Reynolds numbers as high as 3000.

In 1933, J. Nikuradse [7] investigated the relationship between surface

roughness and the pressure loss in pipes. In his research, Nikuradse obtained and classified sand grains of various sizes. He then glued these sand grains to the inside of various pipes to produce a desired roughness and the pressure drop was then determined for different values of Reynolds numbers. In his experiments observations were made on the loss of head (pressure drop), velocity distribution in the test pipe, discharge quantity and the temperature of the water. From this information, Nikuradse was able to determine a relationship between the Reynolds number and the friction factor of the pipe. This relationship had three distinct regions. The first region consisted entirely of laminar flow within the pipe and extended from Reynolds numbers from 0 to 2,000. In this region, the friction factor was related to the Reynolds number by the relationship:

$$f = 64/Re \tag{4}$$

This first region was predicted analytically by Hagen and Poiseuille and was characterized by the linear relationship between the friction factor and the Reynolds number. The second region was termed the transition region and extended from Reynolds numbers of 2,000 to 100,000. The smoother the pipe used for experimentation, the higher the transition Reynolds number. For extremely rough pipes transition occurred at a Reynolds number of 4,000. For extremely smooth pipes, this region would last to Reynolds numbers nearing 100,000. The friction factor in the latter region was related to the Reynolds number by the relationship:

$$f = \frac{0.316}{(Re^{.25})} \tag{5}$$

The final region was classified as the fully rough region and started with Reynolds numbers ranging from 4,000 to 100,000, depending upon the roughness of the pipe. In this region the friction factor was independent of the Reynolds number and was determined using the relationship:

$$f = \frac{1}{(1.74 + 2*(\log r/k))^2} \tag{6}$$

This last region was characterized by the dependence of the friction factor upon the r/k ratio instead of the Reynolds number. This r/k ratio is the inverse of the relative roughness k/r which was used in early experiments. Recently more literature has assigned the relative roughness as e/D. Each notation is found in literature.

The findings of Nikuradse help in the development of semi-empirical theories of fluid friction factors. In 1935, L. Prandtl developed the following formula for the friction factor in turbulent flow in smooth pipes:

$$\frac{1}{\sqrt{f}} = 2.0\log(Re\sqrt{f}) - 0.8 \tag{7}$$

At about the same time, T. von Karmen developed the following relation for friction factor for completely turbulent flow:

$$\frac{1}{\sqrt{f}} = -2.0\log\left(\frac{e/D}{3.7}\right) \tag{8}$$

Both of these relationships are the limited in their application to Nikuradse's work to the completely laminar or completely turbulent region.

In 1939, C. F. Colebrook [8] developed a formula that combined the laminar and turbulent limits and also covered the transition region. This relationship stated:

$$\frac{1}{\sqrt{f}} = -2.0 \log\left(\frac{e/D}{3.7} + \frac{2.51}{Re\sqrt{f}}\right) \tag{9}$$

Colebrook's equation allowed a single relationship to relate the entire range for the friction factor. The drawback to the equation was that the friction factor was implicit with respect to f.

Shortly after Nikuradse and Colebrook published their works, Lewis Moody [9] realized the importance of these findings. In his paper, he plotted the experimental results of Nikuradse and Colebrook. This plot has since been termed the Moody Diagram. The diagram plotted the relationship between the Reynolds number, the friction factor, and the relative roughness of a pipe. If any two of these pieces of information were known, the third could be determined by using the diagram. Since data already existed on the relative roughness of most industrial piping, it was relatively easy to calculate the friction factor that would exist within a pipe for a certain Reynolds number. The Darcy-Weisbach equation:

$$gh_f = f\frac{L}{d}\frac{v^2}{2} \tag{10}$$

where f is the friction factor, v the fluid velocity, L the length of the pipe, d the diameter of the pipe, and g the acceleration due to gravity, may then be used to solve for the resulting head loss in the pipe. The Moody diagram greatly simplified pipe flow calculations and is still in wide use today.

In recent years, many researchers, such as Characklis [10,11,12], Turakhia [3], and Trulear [10] have realized the importance for investigation into the effects of biofouling on fluid dynamics. Many researchers have helped to define the basic processes involved in biofouling. For example, Trulear and Characklis [10], in their work 'Dynamics of Biofilm Processes', helped to define the basic processes occurring in biofouling. Their research found that the processes which contribute to the overall biofilm accumulation are:

1. Organic adsorption.
2. Transport of microbial particles to the surface.
3. Microorganism attachment to the surface.
4. Growth of attached microorganisms.
5. Reentrainment of biofilm by fluid shear.

Strauss and Puckorius [2] recently investigated the different types of fouling occurring in industrial heat exchangers. Their research helped to classify the different types of fouling depositions which may possibly occur within industrial heat exchangers. They investigated three major types of depositions which were precipitation fouling, biological fouling, and corrosion fouling. This work helped to give the reader a better understanding of the processes involved in these types of fouling and possible methods to remove the fouling.

In 1987, Carl Hoerger [13,14] began the study of heat transfer modeling for the control of fouling in heat exchangers. The theoretical work of Hoerger attempted to simulate biofilm parameters, such as growth rates and fouling factors, within a heat exchanger. These analytical simulations were then used to predict actual conditions within a heat exchanger.

## Implications for this Investigation

The findings of the previous investigators were used to determine the basic variables for this experiment. The implications from the previous work are summarized as follows:

1. The major form of fouling currently affecting industrial heat exchangers was biological fouling. Due to that fact, this was the form of fouling that was investigated in this research.

2. The major factor affecting the fluid in the heat exchanger was the surface of the biofilm. Therefore, only the thickness of the biofilm and the surface conditions were investigated in this research. The biofilm characteristics were assumed constant throughout its thickness.

3. Since the important surface characteristics were those of the biofilm, the material of the pipe was unimportant. For this reason, glass tubing was used throughout the experimentation. This was done for ease in the observation and measurement of the biofilm thickness.

4. Since isolation of a single type of film is possible only if the entire system can be sterilized, the biofilm was seeded from microorganisms within the air and in the Bozeman water system. Currently methods such as autoclaving are available for sterilization of some test apparatus, but unfortunately this process is limited to dimensions significantly smaller then the test apparatus used for this experimentation. The water was exposed to air throughout the experimentation to allow any microorganisms present in the air to enter the flow loop. The flow loop was supplied with tap water to allow it to be seeded

with any microorganisms present in the Bozeman water system.

5. The only factor allowed to change the fluid temperature was a change in the temperature of the surrounding room air.

6. The oxygen level would be held constant throughout the investigation. Since the oxygen saturation point is dependent upon temperature, this point would fluctuate slightly as the temperature of the test fluid varied.

7. The nutrient level would be held constant for all of the four test runs in the investigation.

8. For ease in data reduction, the elevation of the entire test section remained the same throughout the investigation.

9. The biofilm thickness was neglected in determining the diameter of the glass in the test section. For all calculations, the diameter of the pipes was assumed constant throughout the research. For data reduction, the biofilm thickness would change the pipe diameter roughly 1 percent at the maximum biofilm thickness.

10. To determine a dimensional correlation, the diameter of the test sections would vary from that of an actual heat exchanger, roughly 7/8 inch diameter, to a diameter of 1/4 inch. This gives a variance in the cross-sectional area of ten, with the maximum area 0.615 square inches and the minimum area 0.0594 square inches.

# CHAPTER 3

# OUTLINE OF INVESTIGATION

## Objectives

The objectives of the experimental research for predictive modeling of a biofilm had two major areas of concern. The first was to investigate the relationship between the friction factor and the biofilm thickness, and the second was to investigate the effect of the biofilm thickness on the heat transfer coefficient. It was felt that by combining these two pieces of information, a predictive model of the biofouling could be determined while the heat exchanger was still in operation. The research for this thesis was concerned primarily with the change in the friction factor as the biofilm grew.

## Scope of the Investigation

During the initial design of the experiment, it was determined that the experimental variables to be investigated should be applicable to the conditions affecting heat exchangers. Therefore, the investigation varied the velocity of the fluid to the point of detachment of the biofilm from the surface of the pipe. Investigation beyond this point was considered unneccesary.

Four separate flow loops were used to determine the relationship between the pipe diameter and the flow parameters. The addition of more than one pipe diameter allowed investigation into the possibility of non-dimensionalizing the final results.

The biofilm thickness in the test section was allowed to vary from an initial condition of no biofilm to a final state of a fully matured biofilm within the test section.

## Facilities and Equipment

All of the experiments and test runs performed were conducted at Montana State University in Ryon Laboratory, Room 21, Laboratory Station 1. The laboratory design consisted of four individual flow loops. All of the flow loops were identical except for the diameter of the pipe used in the entrance length and test section. Figure 1 gives a schematic drawing of one of the flow loops used in the experimentation.

All four flow loops were supplied by a thirty-gallon tank of fluid located on the floor of Ryon Laboratory. The lower tank was placed near the entrance to the test section for ease in operation. The lower tank was lined with plastic to stop corrosion by the biofilm. A pump located on the side of the tank was then used to supply fluid to a suspended tank, which was elevated to a height of approximately thirty feet. This upper tank rested upon a platform which was suspended on top of a support tower located in the laboratory. The

water level in this upper tank was held constant by placing an overflow pipe on the side of the tank. The overflow from this upper tank was then returned to the lower tank to recycle again.

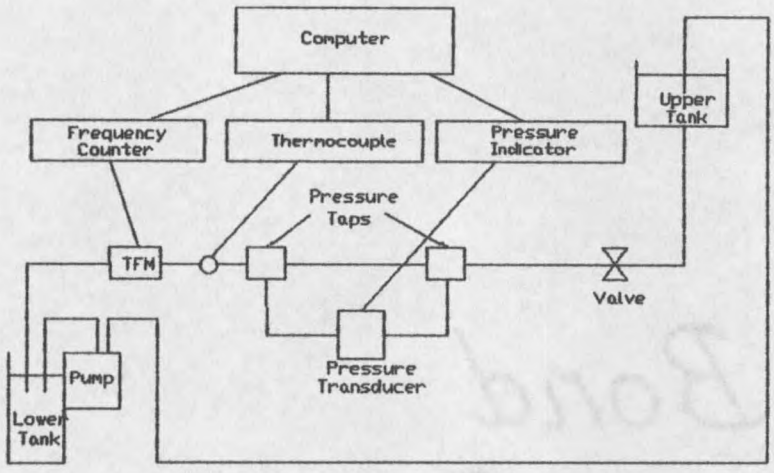


Figure 1. Diagram of Flow Loop and Instrumentation.

Hoses were attached to the bottom of the suspended tank to allow the water in the tank to gravity feed. By placing the tank at an elevation of thirty feet, a wide range of velocities could be measured. The supply hoses consisted of roughly thirty-five feet of 5/8 inch diameter garden hose. This eliminated any possibility of picking up vibrations which may have been caused by the building itself.

Once the hoses reached the support table, they were connected to gate

valves. These valves allowed control of the velocity of the fluid through the hoses. Locating these valves at the beginning of the support table was to reduce the difficulty in operation and access.

After passing the valves, the water entered a bubble trap. Removing the air bubbles from within fluid helped to give a more uniform growth pattern to the biofilm in the test section. The bubble trap consisted of an enlarged pipe tee with a valve located at the top to allow the trapped air to be removed.

After passing the bubble trap, the water was allowed to enter a section of pipe of the same diameter as the test section. This produced an entrance length which allowed the water to reach steady state conditions by the time it reached the test section. The entrance lengths and the length to diameter ratios (L/d) for the flow loops are listed in Table 1.

Table 1. Entrance Length Specifications

| Loop Number | Entrance Length (inches) | Entrance Length Pipe Diameters |
|---|---|---|
| 1 | 40.3 | 75.8 |
| 2 | 44.6 | 111.5 |
| 3 | 45.6 | 149.0 |
| 4 | 47.4 | 169.3 |

The minimum L/D ratio used was 75. According to Incropera and Dewitt [15], the minimum ratio necessary for fully developed conditions is between 10 and 60. Therefore, for all four flow loops fully developed conditions were assumed.

After leaving the entrance length, the test fluid passed through a plastic pressure tap. This pressure tap consisted of five inches of two-inch diameter polycarbonate plastic. Figure 2 gives a drawing of the pressure tap used in the research. The entire length of the plastic tap was bored to the inside diameter of the test pipe, and the first inch and last inch were bored so a brass sleeve could fit into the pressure tap. The sleeves were then sealed to the plastic pressure tap. This design of the pressure taps allowed the glass piping to be placed within the tap while maintaining a constant inside pipe diameter. The brass sleeve allowed the glass test section to be sealed to the plastic pressure tap. This was done by placing plastic tubing over the sleeve and glass test section and clamping. The sleeve was necessary since the plastic tap could not be clamped.

This pressure tap design allowed an average pressure reading to be taken as the fluid entered the test section. The pressure tap took readings from the top, bottom, and from both sides of the pipe and then averaged these readings. This averaged pressure reading was then transmitted to a pressure transducer. The pressure transducer was placed in parallel with the test section by connecting the pressure taps to the transducer with plastic tubing. Plastic tubing was used so that any air not removed by the bubble traps could be detected visually and removed. The pressure transducer was placed on the support table

by the test section and between the pressure taps. These pressure transducers were then attached to pressure indicators. The pressure transducer, pressure indicator, and connectors were calibrated as one unit and kept together throughout the experiment. Appendix B gives the results of the initial and final calibrations, with the resulting accuracies and resolutions.

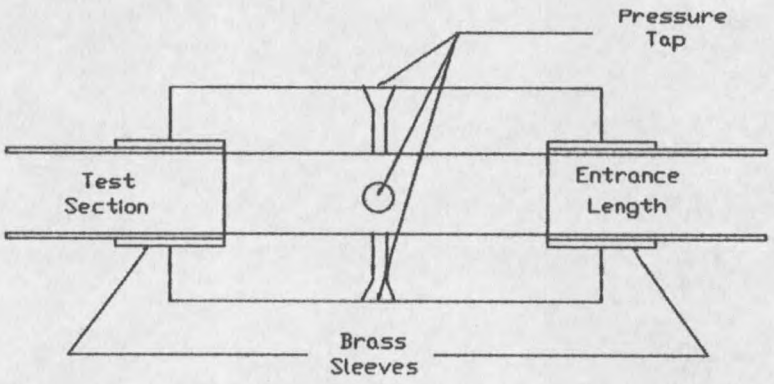


Figure 2. Diagram of Pressure Tap.

After passing the pressure taps, the water entered the glass test section. The test section was designed to be rotated to allow observations to be made on any side of the piping without changing any of the flow characteristics. The lengths and diameters of the test section are listed in Table 2. At the end of the test section the glass piping entered another pressure tap as described above. This allowed the pressure drop across the section to be calculated.

Table 2. Test Section Specifications

| Loop Number | Test Length (inches) | Inside Diameter (inches) | Outside Diameter (inches) |
|---|---|---|---|
| 1 | 35.6 | 0.532 | 0.625 |
| 2 | 36.0 | 0.400 | 0.475 |
| 3 | 36.0 | 0.306 | 0.392 |
| 4 | 36.0 | 0.280 | 0.352 |

Once the water passed the second pressure tap, it entered a six inch length of piping with the same diameter as the test section. The fluid then entered a turbine flow meter. The turbine flowmeter was connected to a frequency counter located on the equipment table. The calibrated turbine flowmeter readings from the frequency counter were used to calculate the velocity of the fluid passing through the test section. Appendix A gives the calibration statistics and the accuracy and resolution of the frequency counter and turbine flowmeters. Immediately after the turbine flowmeter, a T-type thermocouple was installed within the fluid flow. The thermocouple was connected to the computer to allow a constant recording of the temperature of the fluid exiting the test section. This recording could be taken at any time or averaged over a given time period. Tests of the temperature variation along the entire length of the flow loop showed identical temperature readings through all points of the flow loop. Therefore, the temperature probe was placed at the end of the test

section for ease of installation and maintenance. After passing the thermocouple, the fluid entered drain hoses which returned the water to the tank located on the floor.

The valves, entrance lengths, test sections, turbine flowmeters, and thermocouples of all four flow loops were held rigid by mounting the flow loop to a support stand. The support stand was elevated from the table to allow a microscope to be placed underneath the glass test section so that biofilm thickness measurements could be taken with greater ease. The piping was placed in circular plastic rings which were clamped to the support structure. This design lowered the possibility of breaking the glass tubing by reducing the radial movement of the test apparatus. A twenty-four inch viewing section was cut into the support structure underneath the test section to facilitate placing a microscope under the test section.

## Test Matrix

Due to the length of time necessary for a single test run, it was decided during the initial stages of the research that only two major areas of concern were to be investigated. The first area was the characteristics of the initial growth of the biofilm in the test section, the second was the study of the characteristics of the biofilm in the test section during detachment from the pipe wall. It was felt that these two areas would give a much better understanding of biofouling processes occurring in heat exchangers. The test matrix used for the research was split into two areas of investigation. The first test

matrix was called the growth phase, and the second test matrix was termed the detachment phase. Throughout the thesis, the results for both phase will be listed. The test matrix for both phases follows.

For Growth Phase

1. Pressure measurements were taken to determine the pressure drop across the test section. From this information, the friction factor caused by the biofilm in the glass piping could be calculated.
2. Velocity measurements would be taken to determine the wall shear stress on the biofilm in the test section. The velocity would be held constant at 1.00, 1.25, 1.50, and 1.75 ft/sec for test runs one through four respectively. The corresponding Reynolds numbers varied from 2,800 to 17,000
3. The temperature in the test section would be measured to determine the properties of the fluid.
4. The biofilm thickness in the test section would be measured to determine any correlation between the measured variables and the biofilm thickness.
5. Four individual flow loops would be used to determine the effects of the variation of pipe diameter on the results.
6. The oxygen level would be held constant throughout the experimentation. This level would be measured once every twenty-four hours during the test runs.

7. The nutrient level would be held constant throughout the experimentation. It would be determined at the beginning of each of the four test runs for comparison.
8. All data would be recorded at maximum intervals of twelve hours. The time between test points would be reduced as the growth of the biofilm increased.

For Detachment Phase

The second stage of the investigation was the detachment phase. The test matrix for the detachment phase was as follows:

1. The velocity would be varied from the growth velocity to 3 ft/sec.
2. All other pertinent information would be recorded as in the growth phase.

# CHAPTER 4

# PRESSURE MEASUREMENTS

## Experimental Apparatus and Procedures

Pressure readings were taken in all four flow loops using 1.0 psi full scale pressure transducers. Table 14 in Appendix B gives the resolution and accuracy of the pressure transducers used in the experimentation. These measurements were taken for the purpose of determining the friction factor for the biofilm in the test section.

## Friction Factor for Growth Phase

Figures 3 through 6 plot the relationship between the friction factor and test time during the growth phase for flow loops one through four respectively. To make an accurate comparison between data points, it was necessary to plot the friction factor at similar Reynolds numbers. To accomplish this, the relative roughness, e/D, was calculated for the data point. This relative roughness was used to determine the friction factor at a Reynolds number of 10,000. The value of 10,000 for the Reynolds number was chosen arbitrarily. Appendix C gives a description of the exact method used to accomplish this.

As can be seen from the results, the friction factor maintains a constant

value of roughly 0.033 between thirty-six and fifty-seven hours for test velocities of 1.0, 1.25, and 1.50 ft/sec. For a test velocity of 1.75 ft/sec, the friction factor did not change throughout the test run.

After the initiation stage, the friction factor increased linearly in relation to time for approximately one hundred and ninety hours for a test velocity of 1.0 ft/sec, to one hundred hours for a test velocity of 1.50 ft/sec.

Following the growth stage, the increase in the friction factor declined. Data was taken approximately eighteen hours into this plateau stage before the test run was ended. The maximum friction factor ranged from approximately 0.1 for a test velocity of 1.0 ft/sec, to 0.048 for a test velocity of 1.50 ft/sec.